APPENDICES

Appendix A

F Test

Table A-1 F Distribution critical values for 90% confidence

Denominator DF ↓	Numerator DF											
	1	**2**	**3**	**4**	**5**	**6**	**7**	**8**	**9**	**10**	**12**	**15**
1	39.863	49.500	53.593	55.833	57.240	58.204	58.906	59.439	59.858	60.195	60.705	61.220
2	8.526	9.000	9.162	9.243	9.293	9.326	9.349	9.367	9.381	9.392	9.408	9.425
3	5.538	5.462	5.391	5.343	5.309	5.285	5.266	5.252	5.240	5.230	5.216	5.200
4	4.545	4.325	4.191	4.107	4.051	4.010	3.979	3.955	3.936	3.920	3.896	3.870
5	4.060	3.780	3.619	3.520	3.453	3.405	3.368	3.339	3.316	3.297	3.268	3.238
6	3.776	3.463	3.289	3.181	3.108	3.055	3.014	2.983	2.958	2.937	2.905	2.871
7	3.589	3.257	3.074	2.961	2.883	2.827	2.785	2.752	2.725	2.703	2.668	2.632
8	3.458	3.113	2.924	2.806	2.726	2.668	2.624	2.589	2.561	2.538	2.502	2.464
9	3.360	3.006	2.813	2.693	2.611	2.551	2.505	2.469	2.440	2.416	2.379	2.340
10	3.285	2.924	2.728	2.605	2.522	2.461	2.414	2.377	2.347	2.323	2.284	2.244
11	3.225	2.860	2.660	2.536	2.451	2.389	2.342	2.304	2.274	2.248	2.209	2.167
12	3.177	2.807	2.606	2.480	2.394	2.331	2.283	2.245	2.214	2.188	2.147	2.105
13	3.136	2.763	2.560	2.434	2.347	2.283	2.234	2.195	2.164	2.138	2.097	2.053
14	3.102	2.726	2.522	2.395	2.307	2.243	2.193	2.154	2.122	2.095	2.054	2.010
15	3.073	2.695	2.490	2.361	2.273	2.208	2.158	2.119	2.086	2.059	2.017	1.972

Taken from: http://www.statsoft.com/textbook/sttable.html

Table A-2 *F* Distribution critical values for 95% confidence

Denominator DF ↓ / Numerator DF	1	2	3	4	5	6	7	8	9	10	12	15
1	161.448	199.500	215.707	224.583	230.162	233.986	236.768	238.883	240.543	241.882	243.906	245.950
2	18.513	19.000	19.164	19.247	19.296	19.330	19.353	19.371	19.385	19.396	19.413	19.429
3	10.128	9.552	9.277	9.117	9.014	8.941	8.887	8.845	8.812	8.786	8.745	8.703
4	7.709	6.944	6.591	6.388	6.256	6.163	6.094	6.041	5.999	5.964	5.912	5.858
5	6.608	5.786	5.410	5.192	5.050	4.950	4.876	4.818	4.773	4.735	4.678	4.619
6	5.987	5.143	4.757	4.534	4.387	4.284	4.207	4.147	4.099	4.060	4.000	3.938
7	5.591	4.737	4.347	4.120	3.972	3.866	3.787	3.726	3.677	3.637	3.575	3.511
8	5.318	4.459	4.066	3.838	3.688	3.581	3.501	3.438	3.388	3.347	3.284	3.218
9	5.117	4.257	3.863	3.633	3.482	3.374	3.293	3.230	3.179	3.137	3.073	3.006
10	4.965	4.103	3.708	3.478	3.326	3.217	3.136	3.072	3.020	2.978	2.913	2.845
11	4.844	3.982	3.587	3.357	3.204	3.095	3.012	2.948	2.896	2.854	2.788	2.719
12	4.747	3.885	3.490	3.259	3.106	2.996	2.913	2.849	2.796	2.753	2.687	2.617
13	4.667	3.806	3.411	3.179	3.025	2.915	2.832	2.767	2.714	2.671	2.604	2.533
14	4.600	3.739	3.344	3.112	2.958	2.848	2.764	2.699	2.646	2.602	2.534	2.463
15	4.543	3.682	3.287	3.056	2.901	2.791	2.707	2.641	2.588	2.544	2.475	2.403

Taken from: http://www.statsoft.com/textbook/sttable.html

Table A-3 *F* Distribution critical values for 99% confidence

Denominator DF ↓	Numerator DF											
	1	2	3	4	5	6	7	8	9	10	12	15
1	4052.18	4999.50	5403.35	5624.58	5763.65	5858.99	5928.36	5981.07	6022.47	6055.85	6106.32	6157.29
2	98.50	99.00	99.17	99.25	99.30	99.33	99.36	99.37	99.39	99.40	99.42	99.43
3	34.116	30.817	29.457	28.710	28.237	27.911	27.672	27.489	27.345	27.229	27.052	26.872
4	21.198	18.000	16.694	15.977	15.522	15.207	14.976	14.799	14.659	14.546	14.374	14.198
5	16.258	13.274	12.060	11.392	10.967	10.672	10.456	10.289	10.158	10.051	9.888	9.722
6	13.745	10.925	9.780	9.148	8.746	8.466	8.260	8.102	7.976	7.874	7.718	7.559
7	12.246	9.547	8.451	7.847	7.460	7.191	6.993	6.840	6.719	6.620	6.469	6.314
8	11.259	8.649	7.591	7.006	6.632	6.371	6.178	6.029	5.911	5.814	5.667	5.515
9	10.561	8.022	6.992	6.422	6.057	5.802	5.613	5.467	5.351	5.257	5.111	4.962
10	10.044	7.559	6.552	5.994	5.636	5.386	5.200	5.057	4.942	4.849	4.706	4.558
11	9.646	7.206	6.217	5.668	5.316	5.069	4.886	4.744	4.632	4.539	4.397	4.251
12	9.330	6.927	5.953	5.412	5.064	4.821	4.640	4.499	4.388	4.296	4.155	4.010
13	9.074	6.701	5.739	5.205	4.862	4.620	4.441	4.302	4.191	4.100	3.960	3.815
14	8.862	6.515	5.564	5.035	4.695	4.456	4.278	4.140	4.030	3.939	3.800	3.656
15	8.683	6.359	5.417	4.893	4.556	4.318	4.142	4.004	3.895	3.805	3.666	3.522

Taken from: http://www.statsoft.com/textbook/sttable.html

Table A-4 ANOVA result for GNF yield of samples FG

Source of variance	Degree of freedom (*df*)	Sum of squares (*S*)	Variance (*V*)	Variance ratio (*F*)	Percent contribution (%)
Time	2	8.831	4.415	1.911	1.753
C_2H_4/H_2 flow	(2)	(2.563)	*(pooled)*		
Temperature	2	222.102	111.051	48.064	90.551
Error	4	9.241	2.31		7.696
Total	8	240.175			100

Table A-5 ANOVA result for GNF yield of samples NG

Source of variance	Degree of freedom (*df*)	Sum of squares (*S*)	Variance (*V*)	Variance ratio (*F*)	Percent contribution (%)
Time	(2)	(0.063)	*(pooled)*		
C_2H_4/H_2 flow	2	11.749	27.539	11.322	63.741
Temperature	2	5.16	12.096	4.734	26.651
Error	4	0.853			9.608
Total	8				100

Table A-6 ANOVA result for GNF yield of samples LFe

Source of variance	Degree of freedom (*df*)	Sum of squares (*S*)	Variance (*V*)	Variance ratio (*F*)	Percent contribution (%)
Time	2	14.275	7.137	9.79	1.807
C_2H_4/H_2 flow	2	41.942	20.971	28.764	5.708
Temperature	2	651.488	325.744	446.795	91.661
Error	2	1.457	0.728		0.824
Total	8	709.164			100

Table A-7 ANOVA result for GNF yield of samples LNi

Source of variance	Degree of freedom (*df*)	Sum of squares (*S*)	Variance (*V*)	Variance ratio (*F*)	Percent contribution (%)
Time	2	50.656	25.328	8.306	54.631
C_2H_4/H_2 flow	(2)	(5.874)	*(pooled)*		
Temperature	2	18.707	9.353	3.067	15.459
Error	4	12.196	3.049		29.91
Total	8	81.56			100

Appendix B

Analytical equipment for material characterization

The basic steps for all electron microscopes are as below (Central Facility for Electron Microscopy (CFEM), 2003):

a. By using a positive electrical potential, electrons are formed and them accelerated towards the specimen.
b. By using metal apertures and magnetic lenses, the electron stream is confined into thin, focused monochromatic beam.
c. With a magnetic lens the beam is focused onto a sample.
d. The effects due to interaction inside the irradiated sample are detected and later are transformed into an image.

B-1 Scanning electron microscope

The main features of SEM include the electron gun, the magnetic focusing lenses, the sample vacuum chamber and stage region as well as the electronics console containing the control panel, the electronic power supplies and the scanning modules. Usually a solid state energy dispersive X-ray (EDS) detector is attached to the column as an additional tool for characterization (Bindell, 1992).

The working principles of SEM can be based from the electron optics in Figure B-1. In this figure, the virtual source represents the electron gun which produces the monochromatic electrons. There are three types of electron source: thermionic tungsten, Lanthanum Hexaboride (LaB_6), and hot and cold field emission (Bindell, 1992). The electron stream is first condensed by the first condenser lens which limits the amount of current in the beam. In conjunction with the condenser aperture, it eliminates the high-angle electrons from the beam. Next, the second condenser lens forms the electrons into a thin, tight, coherent beam before the objective aperture further eliminates high-angle electrons from the beam. Later, the scan coils sweep the beam in a grid fashion and dwell on points for a certain time as determined by the scan speed. The final lens or objective lens then focuses the scanning beam onto parts of specimen desired. When the beam strikes the specimen, interactions occur

inside the sample. These interactions are detected with various instruments. The instrument counts the number of interactions and displays a pixel on a cathode ray tube (CRT). After that the beam moves to its next dwell points. The process is repeated until the grid scan is completed (Central Facility for Electron Microscopy (CFEM), 2003). Today, SEM comes in different versions such as virtual SEM (VSEM), environmental SEM (ESEM) and field emission (FESEM) which has higher resolution.

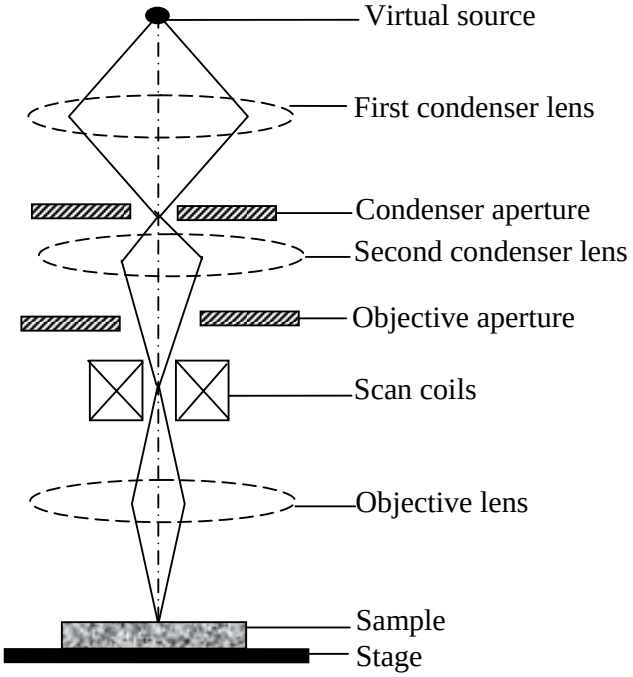

Figure B-1 Schematic of electron optics in SEM (Central Facility for Electron Microscopy (CFEM), 2003)

B-2 Transmission electron microscope

In TEM, the ray of electrons is produced by a pin-shaped cathode heated up by current. The electrons are vacuumed up by a high voltage at the anode with acceleration voltage between 50 and 150 kV. The higher the voltage, the shorter are the electron waves and the higher is the power of resolution (Sengbusch, 2003). The beam of electrons is then focused by the first and second condenser lenses to obtain a small, thin, coherent beam (refer to Figure B-2). The first lens is controlled by the

"spot size knob" in order to determines the "spot size" while the second lens is controlled by the "intensity or brightness knob" that is to change the size of the spot on the sample i.e. from a wide dispersed spot to a pinpoint beam (Central Facility for Electron Microscopy (CFEM), 2003).

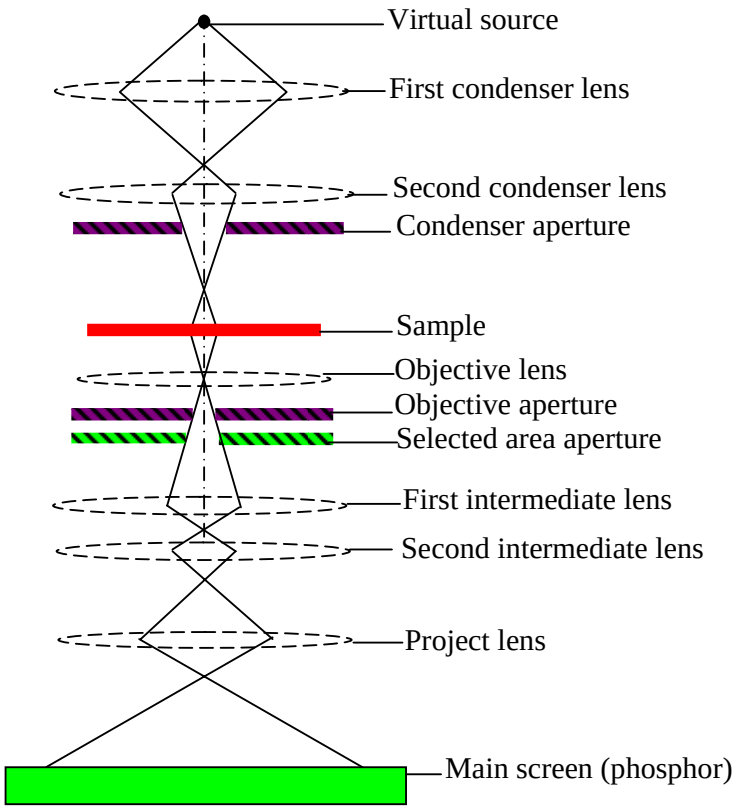

Figure B-2 Schematic of electron optics in TEM (Central Facility for Electron Microscopy, 2003)

After passing through the second condenser lens, the beam is restricted by the condenser aperture just before it strikes the specimen. Here parts of the beam are transmitted and this transmitted portion is focused by the objective lens into an image. The image is enhanced by objective aperture which blocks out high-angle diffracted electrons while selected area aperture enables the user to examine the periodic diffraction of electrons by ordered arrangements of atoms in the sample (Central Facility for Electron Microscopy, 2003). Finally, the image strikes the phosphor image screen and light is generated to allow the user to see the image. The darker regions of the image represent those areas of the sample where more

electrons are scattered (denser or thicker regions in specimen) whereas the lighter regions represent those areas of the sample that more electrons are transmitted through (thinner regions in specimen) (Davis, 2003).

B-3 Raman spectroscopy

There are four major components in Raman spectroscopy. These consist of:

a. Excitation source that is a continuous wave (CW) laser
b. Sample illumination and collection system
c. Wavelength selector that is spectrograph/monochromator
d. Detection and computer control that is CCD

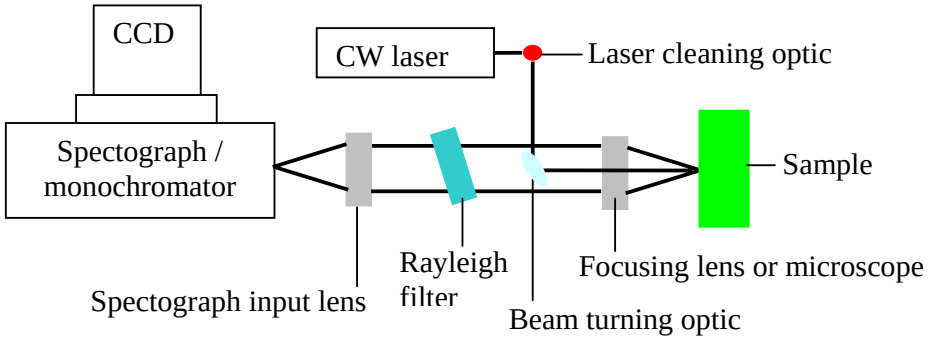

Figure B-3 Schematic diagram of Raman spectroscopy set up (Andor Technology, 2009)

Based from Figure B-3, a sample is illuminated with a laser beam originated from a continuous wave (CW) laser. The light from illuminated spot is collected with a lens and sent through a spectrograph or monochromator. However, wavelengths that are close to the laser line are filtered out by Raleigh filter while the rest of the collected light will be dispersed onto a detector. The detection system consists of dispersive monochromator with a charged couple device (CCD) detector (Ferraro, Nakamoto, & Brown, 2003). CW lasers such as Ar^+ (wavelength between 351.1 – 514.5 nm), Kr^+ (wavelength between 337.4 – 676.4 nm) and He-Ne (wavelength 632.8 nm) are commonly used in Raman spectroscopy. Recently, pulsed lasers such as Nd:YAG (neodymium-doped yttrium aluminium garnet), diode and excimer lasers have been used for time resolved and ultra-violet (UV) resonance Raman spectroscopy (Ferraro et al., 2003). Because Raman scattering is a weak

process, a key requirement to obtain Raman spectra is that the spectrometer provides a high rejection of scattered laser light. New methods such as very narrow rejection filters and Fourier-transform techniques are becoming more widespread (Tissue, 1996).

B-4 X-ray diffractometer

About 95% of all solid materials can be described as crystalline where they exist in crystal form. A crystal is known to possess long-range order because it is composed of atoms arraged in a regular ordered pattern in three dimensions (Suryanarayana & Grant Norton, 1998). When X-rays interact with a crystalline substance, a diffraction pattern is obtained (Scintag Inc., 1999). This can be seen in Figure B-4.

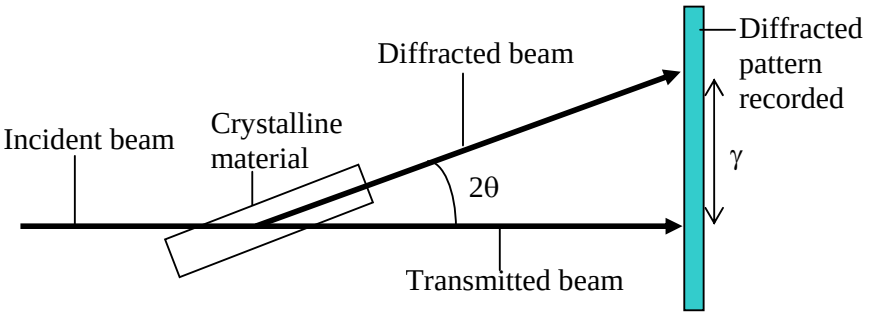

Figure A-4 Diffraction of x-ray by a crystalline material (Moeck, 2004)

The three basic components of XRD are x-ray source, specimen and x-ray detector. These components lie on the circumference of a circle known as focusing circle (Suryanarayana & Grant Norton, 1998) (refer to Figure B-5). The angle between the specimen plane and the x-ray source is known as Bragg's angle, θ while the angle between the projection of the x-ray source and the detector is known as 2θ. The radius of the focusing circle is increases as the angle 2θ decreases. The X-ray radiation most commonly used is that emitted by copper (Cu), whose characteristic wavelength for the Cu Kα radiation is 1.5418Å (Whittingham, 1997)

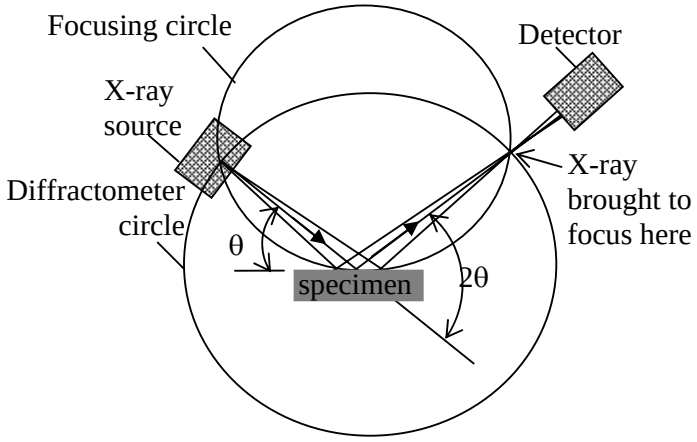

Figure B-5 Geometry of an x-ray diffractometer (Suryanarayana & Grant Norton, 1998)

Appendix C

Experimental and analysis data of the synthesized catalyst, CNTs and GNFs

Table C-1 Catalyst yield (mol%)

Sample	Yield 1	Yield 2	Average
Fe1	98.48	94.45	96.5
Fe2	85.6	90.06	87.8
Fe3	95.23	93.97	94.6
Fe4	91.84	92.09	92.0
Fe5	94.08	86.74	90.4
Fe6	92.76	84.33	88.5
Fe7	77.47	62.89	70.2
Fe8	89	84.33	86.7
Fe9	81.79	73.87	77.8

Sample	Yield 1	Yield 2	Average
Ni1	83.42	84.36	83.9
Ni2	66.86	90.33	78.6
Ni3	86.27	88.44	87.4
Ni4	72.94	84.1	78.5
Ni5	92.5	90.66	91.6
Ni6	76.96	68.78	72.9
Ni7	84.8	86.21	85.5
Ni8	79.1	83.06	81.1
Ni9	78.62	84.88	81.8

Table C-2 Reaction yield of GNFs ($g/(g_{cat}.hr)$)

Sample	Yield 1	Yield 2	Average
1FG	1.074	1.656	1.365
2FG	3.713	4.524	4.119
3FG	2.009	2.529	2.269
4FG	6.590	6.269	6.430
5FG	2.600	2.206	2.403
6FG	1.052	1.105	1.079
7FG	1.847	1.631	1.739
8FG	1.068	1.107	1.088
9FG	3.008	5.971	4.490
1NG	23.948	28.779	26.364
2NG	32.140	28.564	30.352
3NG	20.110	22.947	21.529
4NG	28.842	36.915	32.879
5NG	25.011	26.631	25.821
6NG	19.823	20.786	20.305
7NG	32.956	31.827	32.391
8.NG	24.063	22.367	23.215
9NG	25.100	22.750	23.925

Sample	Yield 1	Yield 2	Average
L_1Fe	1.660	1.860	1.760
L_2Fe	3.062	1.967	2.514
L_3Fe	9.829	10.631	10.230
L_4Fe	1.660	2.930	2.295
L_5Fe	12.280	11.300	11.790
L_6Fe	0.860	0.833	0.847
L_7Fe	12.758	11.370	12.064
L_8Fe	1.267	1.352	1.309
L_9Fe	0.906	0.984	0.945
L_1Ni	51.522	50.676	51.099
L_2Ni	75.707	79.505	77.606
L_3Ni	66.573	68.329	67.451
L_4Ni	48.284	47.100	47.692
L_5Ni	35.934	28.027	31.981
L_6Ni	35.654	37.069	36.361
L_7Ni	43.658	45.650	44.654
L_8Ni	23.755	23.575	23.665
L_9Ni	37.739	42.008	39.873

Table C-3 CNTs specific BET surface area (m^2/g) and true density (g/cm^3)

Sample	Surface area	Density
1R	92.44	2.359
2R	120.80	2.951
3R	64.70	2.703
4R	60.40	2.501
5R	68.99	3.051

Sample	Surface area	Density
6R	70.24	2.623
7R	50.90	2.471
8R	60.70	2.680
9R	56.92	2.590

Table C-4 GNFs specific BET surface area (m^2/g) and true density (g/cm^3)

Preliminary experiment		
Sample	Surface area	Density
1FG	180.15	2.446
2FG	256.80	2.015
3FG	83.88	2.283
4FG	259.05	2.274
5FG	94.47	2.719
6FG	135.30	2.508
7FG	87.52	2.549
8FG	211.40	2.481
9FG	293	2.781
1NG	230.80	1.809
2NG	215.40	2.004
3NG	165.10	2.213
4NG	249.90	1.951
5NG	155.10	2.144
6NG	281.20	2.216
7NG	132.60	2.347
8NG	252.30	1.928
9NG	199.10	1.994

Modified experiment		
Sample	Surface area	Density
L1Fe	127.5	2.624
L2Fe	111.3	2.983
L3Fe	92.56	2.290
L4Fe	195.6	2.301
L5Fe	147.09	2.203
L6Fe	88.08	2.520
L7Fe	146.54	2.087
L8Fe	85.39	2.601
L9Fe	98.31	2.589
L1Ni	291.7	1.927
L2Ni	135.7	1.891
L3Ni	196.9	2.076
L4Ni	139.1	2.148
L5Ni	61.7	2.600
L6Ni	110.95	1.940
L7Ni	60.44	2.237
L8Ni	200.28	1.965
L9Ni	111.54	1.932

Table C-5 -ray diffraction carbon peaks for CNTs and GNFs

Samples	2θ (deg)	d_{002} spacing (Å)
1R	26.31	3.384
2R	26.26	3.39
3R	26.24	3.39
4R	26.30	3.39
5R	26.31	3.39
6R	26.34	3.38
7R	26.29	3.39
8R	26.38	3.38
9R	26.32	3.38
1FG	26.54	3.36
2FG	26.24	3.39
3FG	26.38	3.38
4FG	26.02	3.42
5FG	26.39	3.37
6FG	26.33	3.38
7FG	26.35	3.38

Samples	2θ (deg)	d_{002} spacing (Å)
8FG	26.20	3.40
9FG	26.01	3.42
1NG	26.29	3.39
2NG	26.31	3.38
3NG	26.26	3.39
4NG	26.24	3.39
5NG	26.30	3.39
6NG	26.31	3.38
7NG	26.34	3.38
8NG	26.29	3.39
9NG	26.38	3.38
L1Fe	24.56	3.40
L2Fe	25.12	3.38
L3Fe	24.80	3.39

Samples	2θ (deg)	d_{002} spacing (Å)
L4Fe	23.36	3.40
L5Fe	23.60	3.40
L6Fe	25.12	3.43
L7Fe	22.96	3.39
L8Fe	24.56	3.42
L9Fe	25.20	3.38
L1Ni	25.94	3.43
L2Ni	26.10	3.41
L3Ni	26.07	3.41
L4Ni	25.66	3.47
L5Ni	26.34	3.38
L6Ni	25.87	3.44
L7Ni	26.21	3.40
L8Ni	26.74	3.33
L9Ni	25.90	3.44

Table C-6 Raman spectra bands of CNTs and GNFs (cm^{-1})

Sample	Amorphous (I_A)1500 cm^{-1}	D band intensity (I_D) 1330-1360 cm^{-1}	G band intensity (I_G) 1560-1600 cm^{-1}	Relative value of amorphous to graphite	Degree of graphitization
1R	5.602	9.383	17.725	0.316	0.654
2R	4.423	3.916	8.299	0.533	0.679
3R	5.433	6.268	8.557	0.635	0.577
4R	15.273	16.674	25.344	0.603	0.603
5R	7.357	11.442	28.563	0.258	0.714
6R	3.100	5.135	9.042	0.343	0.638
7R	3.466	3.854	7.762	0.447	0.668
8R	5.051	6.885	20.662	0.244	0.750
9R	13.712	15.487	16.475	0.832	0.515
1FG	8.027	13.417	11.265	0.713	0.456
2FG	10.233	15.418	14.518	0.705	0.485
3FG	11.001	15.403	27.048	0.363	0.407
4FG	7.602	10.238	9.673	0.786	0.486
5FG	10.439	18.826	32.377	0.368	0.309
6FG	8.805	9.347	12.131	0.435	0.726
7FG	7.376	18.624	28.787	0.256	0.607
8FG	8.616	10.202	10.699	0.805	0.512
9FG	7.600	10.749	11.277	0.674	0.512
1NG	34.876	28.103	43.120	0.652	0.553
2NG	12.146	10.752	11.631	0.924	0.489
3NG	16.021	9.983	13.892	0.719	0.464
4NG	12.740	9.203	12.199	0.754	0.489
5NG	28.539	8.346	20.518	0.407	0.418
6NG	10.705	7.658	10.449	0.733	0.494
7NG	11.702	8.896	10.727	0.829	0.478
8NG	12.996	10.445	12.837	0.814	0.497
9NG	12.525	10.272	12.399	0.829	0.498
L1Fe	9.505	12.382	12.550	0.757	0.503
L2Fe	15.561	34.297	39.890	0.390	0.538
L3Fe	11.115	19.627	26.691	0.416	0.576
L4Fe	14.984	22.023	22.830	0.656	0.509
L5Fe	9.597	15.750	16.230	0.591	0.508
L6Fe	9.894	11.579	11.821	0.837	0.505
L7Fe	9.999	18.688	21.011	0.476	0.529
L8Fe	8.653	10.723	10.929	0.792	0.505
L9Fe	13.193	18.325	19.773	0.667	0.519
L1Ni	10.824	13.793	14.080	0.769	0.505
L2Ni	11.600	14.044	14.608	0.794	0.510
L3Ni	12.100	14.962	15.073	0.803	0.502
L4Ni	11.419	14.697	13.843	0.825	0.485
L5Ni	10.735	15.893	16.277	0.660	0.506
L6Ni	11.008	14.376	14.330	0.768	0.499
L7Ni	21.082	33.668	33.965	0.621	0.502
L8Ni	15.782	21.648	21.773	0.725	0.501
L9Ni	13.437	17.156	18.488	0.727	0.519

Note: Relative value of amorphous to graphite = I_A/I_G
Degree of graphitization = $I_G/(I_D+I_G)$

Appendix D

Hydrogen adsorption data

Table D-1 Hydrogen adsorption experimental data at 77 K

	Adsorption		Desorption	
	Pressure (bar)	Uptake (wt%)	Pressure (bar)	Uptake (wt%)
Sample 9FG	0.00	0.1103	19.68	0.6427
	0.03	0.0484	16.01	0.6280
	0.30	0.1894	13.55	0.6112
	1.02	0.3023	10.95	0.5886
	2.50	0.4120	8.94	0.5652
	4.02	0.4672	7.81	0.5497
	5.53	0.5040	6.88	0.5345
	7.07	0.5311	5.89	0.5150
	8.59	0.5593	4.91	0.4916
	9.94	0.5721	4.00	0.4647
	11.67	0.5951	2.41	0.3993
	13.16	0.6043	1.40	0.3245
	14.12	0.6108	0.97	0.2667
	15.15	0.6174	0.50	0.1751
	16.61	0.6256	0.10	0.0516
	18.14	0.6340	0.01	0.0293
	20.14	0.6423		
Sample 4NG	0.02	0.0012	20.11	0.5809
	0.30	0.1230	20.01	0.5842
	1.02	0.2259	16.03	0.5571
	2.54	0.3186	13.55	0.5339
	4.05	0.3717	11.04	0.5070
	5.55	0.4094	9.02	0.4802
	7.06	0.4395	7.99	0.4646
	8.55	0.4649	6.96	0.4468
	10.08	0.4878	6.00	0.4277
	11.96	0.5041	4.90	0.4032
	13.15	0.5174	3.97	0.3783
	14.10	0.5250	2.50	0.3265
	15.13	0.5371	1.39	0.2651
	16.59	0.5520	0.98	0.2317
	18.10	0.5635	0.47	0.1665
	20.11	0.5809	0.09	0.0643
			0.01	0.0206

	Adsorption		Desorption	
	Pressure (bar)	Uptake (wt%)	Pressure (bar)	Uptake (wt%)
Commercial SWNT	0.00	0.1490	20.10	1.0675
	0.02	0.0560	20.03	1.0693
	0.30	0.2602	16.07	1.0257
	1.02	0.4638	13.57	0.9914
	2.52	0.6382	10.95	0.9454
	4.04	0.7326	8.73	0.8983
	5.52	0.7941	8.00	0.8807
	7.06	0.8437	7.01	0.8536
	8.53	0.8820	5.97	0.8215
	10.08	0.9178	4.90	0.7815
	11.58	0.9508	4.01	0.7406
	12.88	0.9694	2.49	0.6456
	14.18	0.9905	1.36	0.5266
	15.14	1.0048	0.97	0.4606
	16.61	1.0230	0.48	0.3376
	18.11	1.0429	0.09	0.1433
	20.10	1.0675	0.01	0.0912

Table D-2 Hydrogen adsorption experimental data at 298 K

	Adsorption		Desorption	
	Pressure (bar)	Uptake (wt%)	Pressure (bar)	Uptake (wt%)
Sample 9FG	0	0.0000	137.2	0.2957
	10.05	0.0941	130.85	0.2918
	19.97	0.1196	120.03	0.2830
	30.03	0.1404	109.97	0.2659
	39.98	0.1609	100.1	0.2517
	49.98	0.1786	90.12	0.2412
	59.99	0.1984	80.04	0.2294
	70.03	0.2120	70.23	0.2081
	80.04	0.2259	59.76	0.2003
	89.96	0.2356	49.99	0.1771
	100.04	0.2523	40.01	0.1551
	109.98	0.2634	30.01	0.1400
	120.11	0.2785	20.00	0.1179
	130.51	0.2911	9.98	0.0858
	137.17	0.2939	8.91	0.0791
			7.98	0.0734
			7.00	0.0705
			5.98	0.0667
			3.98	0.0522
			2.98	0.0496
			2.00	0.0432
			1.05	0.0283
Sample L6Ni	0.00	0.0000	89.67	0.0662
	1.99	0.0344	79.65	0.0678
	3.99	0.0385	69.69	0.0646
	5.99	0.0381	59.68	0.0638
	10.00	0.0324	49.67	0.0636
	19.95	0.0395	39.68	0.0556
	39.68	0.0500	29.63	0.0534
	49.68	0.0612	19.57	0.0462
	59.70	0.0549	10.00	0.0389
	69.73	0.0601	8.00	0.0417
	79.68	0.0574	5.99	0.0420
	89.70	0.0591	3.99	0.0227
	99.65	0.0665		
	0.00	0.0000		

	Adsorption		Desorption	
	Pressure (bar)	Uptake (wt%)	Pressure (bar)	Uptake (wt%)
Sample L7Ni	0	0.0000	150.18	0.0938
	1.03	0.0029	140.00	0.0914
	2.8	0.0062	130.02	0.0863
	3.96	0.0066	120.08	0.0823
	4.97	0.0078	110.06	0.0779
	6.04	0.0085	100.27	0.0747
	6.94	0.0102	90.12	0.0693
	7.98	0.0106	79.99	0.0632
	9.07	0.0104	69.99	0.0581
	9.90	0.0120	59.91	0.0525
	19.94	0.0211	49.91	0.0447
	30.35	0.0278	40.00	0.0381
	39.97	0.0380	29.91	0.0299
	49.82	0.0444	19.88	0.0210
	59.97	0.0507	9.98	0.0125
	69.99	0.0565	9.00	0.0110
	79.70	0.0641	7.98	0.0109
	90.04	0.0683	6.99	0.0083
	100.04	0.0728	6.00	0.0070
	110.04	0.0766	4.96	0.0051
	120.09	0.0827	3.96	0.0047
	130.01	0.0862	2.98	0.0029
	139.99	0.0897	1.96	0.0012
	150.18	0.0938		
Sample L7Fe	0.00	0.0000	89.70	0.1800
	0.99	0.0425	79.69	0.1738
	5.00	0.0579	69.73	0.1661
	10.00	0.0731	59.72	0.1515
	19.95	0.0985	49.67	0.1380
	29.62	0.1113	39.71	0.2404
	39.67	0.1362	29.65	0.1016
	49.66	0.1530	19.58	0.0793
	59.66	0.1620	0.99	0.0182
	69.68	0.1743	89.70	0.1800
	79.64	0.1846	79.69	0.1738
	89.67	0.1943	69.73	0.1661
	99.65	0.2037	59.72	0.1515

Table D-2 Hydrogen adsorption experimental data at 298 K (continued)

	Adsorption		Desorption	
Sample 4NG	Pressure (bar)	Uptake (wt%)	Pressure (bar)	Uptake (wt%)
	0.00	0.0000	149.99	0.0567
	2.66	0.0017	140.00	0.0556
	5.00	0.0050	130.03	0.0542
	9.00	0.0078	120.11	0.0525
	9.86	0.0080	110.03	0.0508
	20.02	0.0133	99.98	0.0476
	30.00	0.0176	90.12	0.0449
	39.90	0.0246	80.00	0.0409
	49.98	0.0280	70.04	0.0369
	59.99	0.0321	60.32	0.0325
	69.92	0.0367	49.99	0.0284
	80.01	0.0407	39.99	0.0247
	90.10	0.0447	29.94	0.0179
	100.00	0.0476	20.01	0.0134
	110.00	0.0506	10.00	0.0089
	120.15	0.0517	9.00	0.0086
	129.99	0.0539		
	140.00	0.0554		
	149.99	0.0567		

	Adsorption		Desorption	
Sample L5Fe	Pressure (bar)	Uptake (wt%)	Pressure (bar)	Uptake (wt%)
	1.99	0.0322	89.66	0.1226
	3.99	0.0454	79.65	0.1136
	6.00	0.0531	69.70	0.1101
	8.00	0.0484	59.69	0.1053
	10.00	0.0547	49.68	0.0944
	19.95	0.0680	39.69	0.0857
	29.61	0.0828	29.64	0.0782
	39.66	0.0959	19.57	0.0659
	44.49	0.0970	10.00	0.0506
	49.65	0.1043	8.01	0.0499
	59.65	0.1081	6.00	0.0462
	69.68	0.1134	3.99	0.0389
	79.63	0.1227	1.99	0.0396
	89.65	0.1296		
	99.62	0.1315		

Appendix E

Prediction of hydrogen isotherm using Neuro-fuzzy system

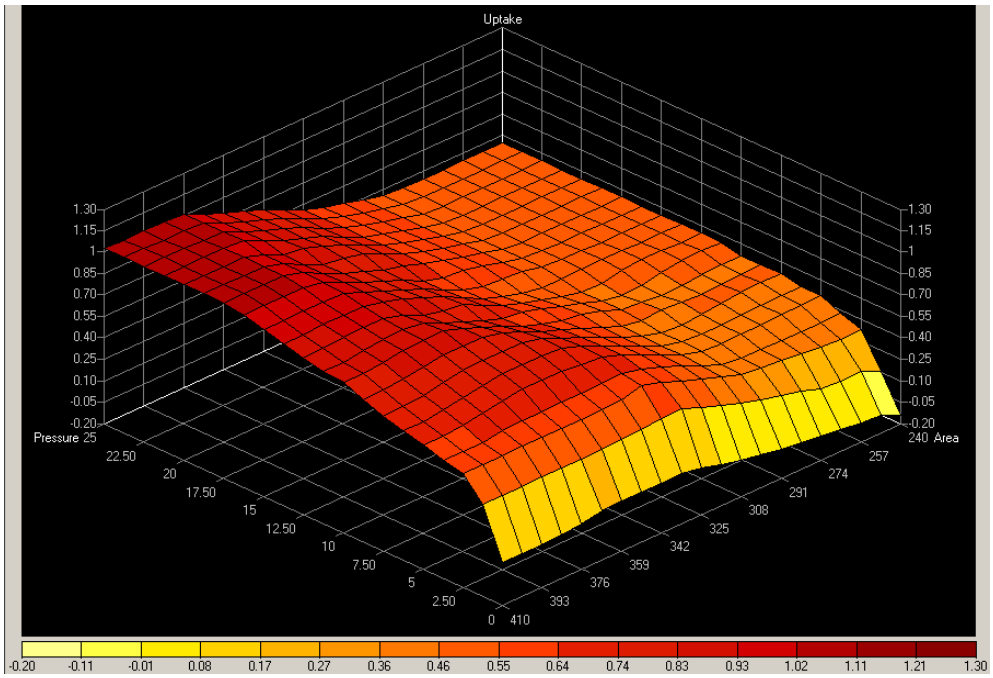

Figure E-1 3-D plot of hydrogen isotherm at 77 K and 20 bar.

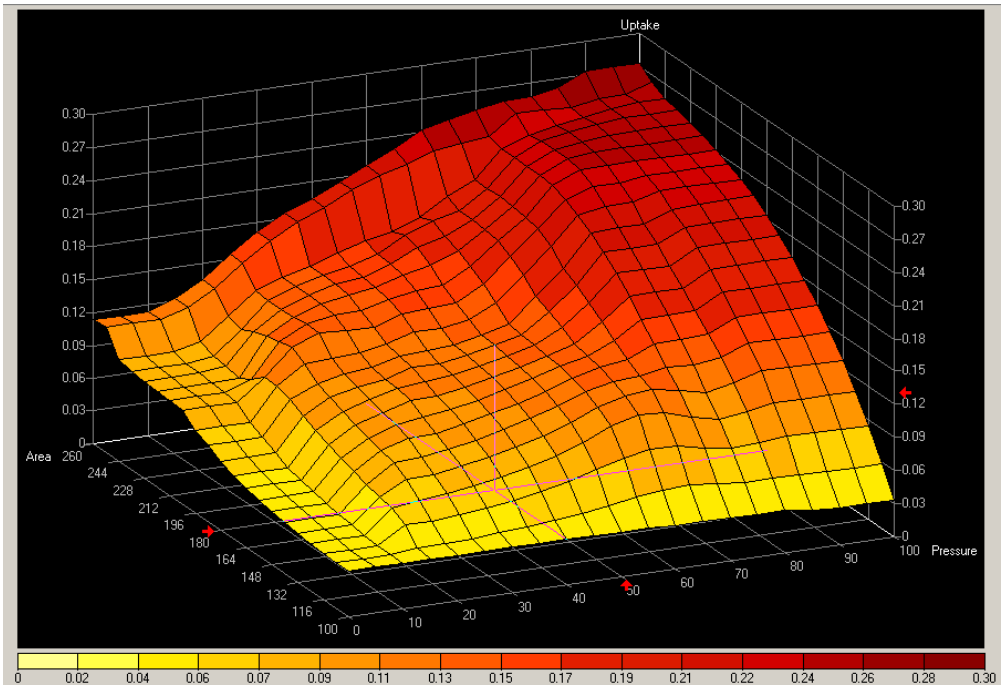

Figure E-2 3-D plot of hydrogen isotherm at 298 K and 100 bar.

Appendix F

List of publications, presentations and research participations

Journal Publications

1. S. Sufian, S. Yusup, G. S. Walker and A. M. Shariff, *Synthesis of graphitic nanofibres using iron (III) oxide catalyst for hydrogen storage application*, Materials Research Innovations, Volume 13, Issue 3, September Special Issue, 2009, pg 153-156.
2. S. Sufian, S. Yusup, G. Walker, T. Murugesan, *Synthesis and characterization of nanosized Fe_2O_3 and NiO at different temperature by precipitation method*, Volume 45, Issue 3, June 2009, Indian Ceramic Review.
3. Suriati Sufian, Suzana Yusup, *Optimization for Development of Carbon Nanotubes using Taguchi Method at Constant Temperature*. Accepted by Journal of Nano Research.
4. Suriati Sufian, Suzana Yusup, Azmi M Shariff, *Hydrogen adsorption of graphitic - nanofibers at high pressure using magnetic suspension balance.* In review by Journal of Applied Science.

National conference

1. Suriati Sufian, *Synthesis of Nanosized Fe_2O_3 and NiO Catalyst by Percipitation Method*, National Postgraduate Conference on Engineering, Science and Technology (NPC) 31 March 2008, UTP, Tronoh.

International Conferences

1. Suriati Sufian, Suzana Yusup, *Hydrogen Adsorption Model Using Neuro-fuzzy System*, Proceedings of the 5th WSEAS International Conference on Data Networks, Communications & Computers, 16-17 October, 2006, Bucharest, Romania.
2. S. Sufian, S. Yusup, G. S. Walker and A. M. Shariff, *Synthesis of graphitic nanofibres using iron (III) oxide catalyst for hydrogen storage application*, International Conference on Functional Material and Devices 2008 (ICFMD), 16-19 June 2008, KL.

3. Suriati Sufian, Suzana Yusup, *Synthesis and Characterization of Graphitic Nanofibres on Unsupported NiO*, The Trinidad and Tobago Gas Conference (TGTC), 7-10 October 2008, Tobago, Republic of Trinidad & Tobago.
4. Suriati Sufian, Suzana Yusup, *Optimization for Development of Carbon Nanotubes using Taguchi Method at Constant Temperature*, The 5th International Conference on Diffusion in Solids and Liquids (DSL 2009), 24-26 June 2009, Rome, Italy.
5. Suriati Sufian, Suzana Yusup, Azmi M Shariff, *Hydrogen adsorption of graphitic nanofibers at high pressure using magnetic suspension balance*, 3rd International Conference On Chemical & Bioprocess Engineering (ICCBPE-2009) - 23rd Symposium Of Malaysian Chemical Engineers (SOMChE-2009), 12-14 August 2009, Kota Kinabalu, Sabah.

PhD research participations and achievements

1. Shell Inter-varsity Student Paper Contest 2008 (S-SPEC), 3-4 March 2008, Universiti Teknologi Malaysia, Skudai – *1st Runner Up in Postgraduate Oral Presentation.*
2. Engineering Design Exhibition (EDX 21), 16-17th April 2008, UTP – *Gold for Chemical Engineering Postgraduate, Winner of the Best Postgraduate Presenter, 1st Runner Up for the Best Postgraduate Poster and 2nd Runner Up for the Most Innovative Award.*
3. 19th International Invention Innovative and Technology Exhibition (ITEX 2008), Kuala Lumpur Convention Centre, 9-11 May 2008.
4. The invention and New Product Exposition (INPEX), 11-14 June 2008, Pittsburgh, USA – *Two Gold Medals in Manufacturing and Chemicals categories.*
5. BASF International summer course, Ludwigshafen, Germany, 21 July – 2 August 2008.
6. Malaysia Technology Exhibition (MTE 2009), 19-21 February 2009, PWTC KL, *Silver medal*.